Titanium and Zirconium Benzyl Complexes Bearing Bulky Bis(amido)cyclodiphosph(III)azanes: Synthesis, Structure, Activation, and Ethene Polymerization Studies

Kirill V. Axenov,[†] Ilkka Kilpeläinen,[‡] Martti Klinga,[†] Markku Leskelä,[†] and Timo Repo*,[†]

Laboratory of Inorganic Chemistry, Department of Chemistry, University of Helsinki, PO Box 55, FIN-00014, Finland, and Laboratory of Organic Chemistry, Department of Chemistry, University of Helsinki, PO Box 55, FIN-00014, Finland

Received August 22, 2005

Benzyl-substituted bis(amido)cyclodiphosph(III)azane complexes $[(RN)(t\text{-BuNP})]_2M(CH_2Ph)_nCl_{2-n}$ (M = Zr, Ti; $n = 1, 2$) bearing *t*-Bu or bulky aryl substituents on amido nitrogens were prepared by direct alkylation of corresponding dichloro derivatives with $PhCH_2MgCl$. The alkylation of Zr complexes proceeded selectively. In the solid state of $[(t\text{-BuN})(t\text{-BuNP})]_2Zr(CH_2Ph)_2$ the zirconium atom adopts a distorted trigonal-bipyramidal configuration. The alkylation of $[(t\text{-BuN})(t\text{-BuNP})]_2TiCl_2$ with $PhCH_2MgCl$ in the presence of THF led to $[(t\text{-BuN})(t\text{-BuNP})]_2Ti(CH_2Ph)_2$ simultaneously with $[(t\text{-BuN})(t\text{-BuNP})]_2Ti(CHPh)(THF)$. According to NMR and X-ray single-crystal studies, the latter contains a Ti−C double bond. Activation of the benzyl complexes with $B(C_6F_5)_3$ led to the generation of the corresponding "cationic" species, which were further investigated by ^1H, ^{13}C, ^{31}P, and ^{19}F NMR methods. In the solid state the metal center of $\{[(t\text{-BuN})(t\text{-BuNP})]_2Zr(\eta^2\text{-}CH_2Ph)(Et_2O)\}^+[PhCH_2B(C_6F_5)_3]^-$ has a distorted trigonal bipyramidal configuration, where the benzyl group coordinates to Zr in a η^2-fashion. In ethene polymerization the mono- and dibenzyl Ti and Zr derivatives showed moderate to high catalytic activities (up to 4600 kg/(mol × h)). The correlation between polymerization results and activation experiments, especially in terms of electrophilicity of the metal center, is discussed.

Introduction

During the last decades non-cyclopentadienyl complexes of group 4 metals have attracted considerable attention as potential catalyst precursors for the homogeneous Ziegler−Natta olefin polymerization process.[1] Besides the recently discovered highly active bis(phenoxyimino) titanium and zirconium catalysts,[2] group 4 metal complexes bearing bi-, tri-, or polydentante amido ligands are promising candidates for catalyst precursors.[3] A highly electrophilic metal cation, $[(R_2N)_2MR]^+$ (M = group 4 metal), which is generally considered as the catalytically active species in olefin polymerization, is generated after methylalumoxane (MAO) activation of bis(amido) complexes.[1a] Owing to the variety of easily synthesized amido ligands, the possibility to modify the electronic character at the metal center as well as its geometry and steric protection is tempting. In this context, we have developed synthetic methods to modify the literature known $[(t\text{-BuN})(t\text{-BuNP})]_2^{2-}$ ligand framework[4] by bulky alkyl and aryl substituents.[5] In our studies a series of dichloro Ti and Zr complexes bearing bulky bis(amido)cyclodiphosph(III)azanes were prepared, and moderate to high catalytic activities in ethene polymerization were recorded after MAO activation.[5,6] It was concluded that the polymerization behavior of these catalysts and the stability of the active species depend on the bulkiness of the amido substituents.[6]

Structural investigations in solution and in the solid state of the cationic species generated from dimethyl hafnium bis(amido)cyclodiphosph(III)azanes by activation with tris(perfluorophenyl)borane have provided further understanding of how the nature and size of the amido substituents influence the activation process as well as the geometry of the metal center when the cationic species are formed.[7] However, unambiguous correlations between the structure of the cationic metal center, polymerization activity, and polymer properties could not be established due to the exhibited low activity of the investigated hafnium complexes. Evidently, the study of the cationic species generated from more catalytically active Ti and Zr cyclodiphos-

* To whom correspondence should be addressed. E-mail: Timo.Repo@helsinki.fi. Fax: +358-(0)9-19150198.

[†] Laboratory of Inorganic Chemistry.

[‡] Laboratory of Organic Chemistry.

(1) (a) Britovsek, J. P.; Gibson, V. C.; Wass, D. F. *Angew. Chem.* **1999**, *111*, 448; *Angew. Chem., Int. Ed.* **1999**, *38*, 428. (b) Gibson, V. C.; Spitzmesser, K. *Chem. Rev.* **2003**, *103*, 283.

(2) (a) Matsui, S.; Mitani, M.; Saito, J.; Tohi, Y.; Makio, H.; Matsukawa, N.; Takagi, Y.; Tsuru, K.; Nitabaru, M.; Nakano, T.; Tanaka, H.; Kashiwa, K.; Fujita, T. *J. Am. Chem. Soc.* **2001**, *123*, 6847. (b) Lamberti, M.; Pappalardo, D.; Zambelli, A.; Pellechia, C. *Macromolecules* **2002**, *35*, 658. (c) Mitani, M.; Mohri, J.; Yoshida, Y.; Saito, J.; Ishii, S.; Tsuru, K.; Matsui, S.; Furuyama, R.; Nakano, T.; Tanaka, H.; Kojoh, S.; Matsugi, T.; Kashiwa, N.; Fujita, T. *J. Am. Chem. Soc.* **2002**, *124*, 3327. (d) Furuyama, R.; Saito, J.; Ishii, S.; Mitani, M.; Matsui, S.; Tohi, Y.; Makio, H.; Matsukawa, N.; Tanaka, H.; Fujita, T. *J. Mol. Catal., Ser. A: Chem.* **2003**, *200*, 31.

(3) (a) Schrock, R. R.; Adamchuk, J.; Ruhland, K.; Lopez, L. P. H. *Organometallics* **2005**, *24*, 857. (b) Mehrkhodavandi, P.; Schrock, R. R. *J. Am. Chem. Soc.* **2001**, *123*, 10746. (c) Scollard, J. D.; McConville, D. H. *J. Am. Chem. Soc.* **1996**, *118*, 10008. (d) Lee, C. H.; La, Y.-H.; Park, J. W. *Organometallics* **2000**, *19*, 344. (e) Horton, A. D.; de With J.; van der Linden, A. J.; van de Weg, H. *Organometallics* **1996**, *15*, 2672. (f) Kim, S.-J.; Jung, I. N.; Yoo, B. R.; Kim, S. H.; Ko, J.; Byun, D.; Kang, S. O. *Organometallics* **2001**, *20*, 2136. (g) Male, N. A. H.; Thornton-Pett, M.; Bochmann, M. *Dalton Trans.* **1997**, 2487.

(4) (a) Grocholl, L. P.; Stahl, L.; Staples, R. J. *Chem. Commun.* **1997**, 1465. (b) Moser, D. F., Carrow, C. J.; Stahl, L.; Staples, R. J. *J. Chem. Soc., Dalton Trans.* **2001**, 1246. (c) Moser, D. F.; Grocholl, L.; Stahl, L.; Staples, R. J. *J. Chem. Soc., Dalton Trans.* **2003**, 1402.

(5) Axenov, K. V.; Klinga, M.; Leskelä, M.; Kotov, V. V.; Repo, T. *Eur. J. Inorg. Chem.* **2004**, 695.

(6) Axenov, K. V.; Klinga, M.; Leskelä, M.; Kotov, V. V.; Repo, T. *Eur. J. Inorg. Chem.* **2004**, 4702.

(7) Axenov, K. V.; Klinga, M.; Leskelä, M.; Repo, T. *Organometallics* **2005**, *24*, 1336.

10.1021/om050725h CCC: $33.50
Publication on Web 12/14/2005

ph(III)azane complexes would be beneficial to gain more information about the relationship between the structure of the catalyst and its polymerization behavior. Here we report on the synthesis of benzyl bis(amido)cyclodiphosph(III)azane Ti and Zr complexes, their activation with $B(C_6F_5)_3$, and their use in homogeneous ethene polymerization.

Experimental Section

General Procedures. All manipulations were performed under inert argon atmosphere using standard Schlenk techniques. The hydrocarbon and ether solvents were refluxed over sodium and benzophenone, distilled, and stored under inert atmosphere with pieces of sodium. C_6D_6 was refluxed over sodium, CD_2Cl_2 and C_6D_5Br were refluxed with CaH_2, and then these solvents were transferred into storage flasks by evaporation−condensation in a vacuum and stored in a glovebox. EI-mass spectra were measured on a JEOL SX102 spectrometer. ESI-HRMS spectra were performed with a Bruker-MicroTOF spectrometer. The ^{1}H, ^{13}C, ^{31}P, and ^{19}F NMR spectra were recorded on Varian Gemini 200 MHz, Varian INOVA 500, and Bruker AMX 400 spectrometers. The ^{1}H and ^{13}C NMR spectra were referenced relative to $CHDCl_2$ (5.28 and 53.73 ppm, respectively), C_6D_4HBr (7.29 and 122.25 ppm, respectively), and C_6D_5H (7.24 and 128.0 ppm, respectively). Phosphorus signals were referenced relative to an external standard (85% H_3PO_4 solution) and external Me_3P solution in CD_2Cl_2 (−60.5 ppm); fluorine signals were referenced relative to $CFCl_3$ standard and external $B(C_6F_5)_3$ in CD_2Cl_2 (−127.8, −143.4, −160.6 ppm). Elemental analyses were performed at Prof. Dr. H. Malissa und G. Reuter GmbH, Germany. High-temperature gel permeation chromatography of polyethylene samples (GPC) was performed in 1,2,4-trichlorobenzene at 145 °C using a Waters HPLC 150C.

tert-Butylamine and phosphorus trichloride were purchased from Merck and purified by distillation under argon (*t*-$BuNH_2$ over sodium hydroxide). Arylamines were received from Aldrich and distilled in vacuo over sodium hydroxide before use. Chlorotrimethylsilane was purchased from Fluka and used as received. Ti(NMe$_2$)$_4$ and Zr(NMe$_2$)$_4$ were purchased from Aldrich and used as a toluene solution. A 1 M solution of $PhCH_2MgCl$ in Et_2O, a 2 M solution of $PhCH_2MgCl$ in THF, and a 1.6 M solution of *n*BuLi in hexane were purchased from Aldrich and used as received. Tris(perfluorophenyl)borane was purchased from Strem and stored in a glovebox. Methylalumoxane (MAO, 30 wt % solution in toluene) was received from Borealis Polymers Oy. [(*t*-BuN)(*t*-BuNP)]$_2$TiCl$_2$ (**1**),[4b,5] [(2,5-*t*-Bu$_2$C$_6$H$_3$N)(*t*-BuNP)]$_2$TiCl$_2$ (**2**),[5] [(2,6-*i*-Pr$_2$C$_6$H$_3$N)(*t*-BuNP)]$_2$TiCl$_2$ (**3**),[5] [(*t*-BuN)(*t*-BuNP)]$_2$ZrCl$_2$ (**9**),[4c] [(2,5-*t*-Bu$_2$-C$_6$H$_3$N)(*t*-BuNP)]$_2$ZrCl$_2$ (**10**),[6] and [(2,6-*i*-Pr$_2$C$_6$H$_3$N)(*t*-BuNP)]$_2$-ZrCl$_2$ (**11**)[6] were prepared according to literature procedures.

Synthesis of Complexes. [(*t*-BuN)(*t*-BuNP)]$_2$Ti(CH$_2$Ph)Cl (4). $PhCH_2MgCl$ in Et_2O (1 M, 3 mL, 3 mmol) was added via a syringe into a solution of [(*t*-BuN)(*t*-BuNP)]$_2$TiCl$_2$ (**1**) (0.7 g, 1.5 mmol) in Et_2O (30 mL) at −50 °C. The reaction mixture was allowed to warm to room temperature and stirred overnight. All volatiles were removed in vacuo, and the resulting red-brown residue was extracted by hexane (20 + 10 mL) followed by filtration in a glovebox through PTFE filters. The clear hexane filtrate was then evaporated in vacuo to give a red solid (0.43 g; 55.0%) ($C_{23}H_{43}N_4P_2TiCl$ calcd C, 53.03; H, 8.32, found C, 53.47; H, 7.87). ^{1}H NMR (400 MHz, C_6D_6, 31 °C): δ_H 1.23 (t, J_{HH} = 0.9 Hz, 9H, *t*-Bu, P_2N_2 cycle), 1.25 (s, 9H, *t*-Bu, P_2N_2 cycle), 1.71 (t, J_{HH} = 0.9 Hz, 18H, *t*-Bu), 2.82 (s, 2H, CH_2Ph), 7.03 (t, J_{HH} = 7.35 Hz, 1H, Ph), 7.33 (t, J_{HH} = 7.35 Hz, 2H, Ph), 7.51 (d, J_{HH} = 7.8 Hz, 2H, Ph). ^{13}C{^{1}H} NMR (50.3 MHz, C_6D_6, 29 °C): δ_C 31.66 (t, J_{PC} = 6.5 Hz, *C*H$_3$, *t*-Bu, P_2N_2 cycle), 34.30 (d, J_{PC} = 12.2 Hz, *C*H$_3$, *t*-Bu), 55.67 (t, J_{PC} = 14.9 Hz, *C*, *t*-Bu, P_2N_2 cycle), 63.9 (d, J_{PC} = 14.5 Hz, *C*, *t*-Bu), 91.76 (*C*H$_2$Ph), 123.05 (Ph), 126.16 (Ph), 128.75 (Ph), 148.72 (Ph). ^{31}P{^{1}H} NMR (162 MHz, C_6D_6, 31 °C): δ_P 110.69 (s). MS(EI): *m*/*z* (%) 521 (43, M$^+$), 429 (32, M$^+$ − CH_2Ph), 347 (78, ligand).

[(*t*-BuN)(*t*-BuNP)]$_2$Ti(CH$_2$Ph)$_2$ (5). $PhCH_2MgCl$ in THF (2 M, 5.5 mL, 11 mmol) was added via a syringe into a solution of [(*t*-BuN)(*t*-BuNP)]$_2$TiCl$_2$ (**1**) (2.4 g, 5.16 mmol) in Et_2O (30 mL) at −50 °C. The reaction mixture was allowed to warm to room temperature and stirred overnight. All volatiles were removed in vacuo, and the resulting red-brown residue was extracted by hexane (20 + 10 mL) followed by filtration in a glovebox through PTFE filters. After precipitation of complex **6**, the hexane phase was separated and evaporated in vacuo to give a red solid (1.2 g; 41.0%). ^{1}H NMR (200 MHz, C_6D_6, 29 °C): δ_H 1.23 (s, 18H, *t*-Bu, P_2N_2 cycle), 1.70 (s, 18H, *t*-Bu), 3.36 (s, 4H, CH_2Ph), 6.96−7.21 (m, 10H, Ph). ^{1}H NMR (500 MHz, CD_2Cl_2, 27 °C): δ_H 1.16 (s, 18H, *t*-Bu, P_2N_2 cycle), 1.55 (s, 18H, *t*-Bu), 3.03 (s, 4H, CH_2Ph), 6.92 (d, J_{HH} = 7.8 Hz, 2H, Ph), 7.06 (t, J_{HH} = 7.8 Hz, 2H, Ph), 7.15 (m, J_{HH} = 7.8 Hz, 4H, Ph), 7.24 (t, J_{HH} = 7.8 Hz, 2H, Ph). ^{13}C-{^{1}H} NMR (50.3 MHz, C_6D_6, 29 °C): δ_C 29.28 (t, J_{PC} = 6.9 Hz, *C*H$_3$, *t*-Bu, P_2N_2 cycle), 34.41 (d, J_{PC} = 11.06 Hz, *C*H$_3$, *t*-Bu), 54.00 (t, J_{PC} = 14.1 Hz, *C*, *t*-Bu, P_2N_2 cycle), 63.9 (d, J_{PC} = 17.9 Hz, *C*, *t*-Bu), 77.24 (*C*H$_2$Ph), 122.76 (Ph), 129.37 (Ph), 129.66 (Ph), 145.33 (Ph). ^{31}P{^{1}H} NMR (202 MHz, CD_2Cl_2, 27 °C): δ_P 129.66 (s). MS(EI): *m*/*z* (%) 576 (3, M$^+$), 485 (11, M$^+$ − CH_2Ph), 347 (89, ligand). HRMS (ESI): found *m*/*z* 577.3 ($C_{30}H_{51}N_4P_2Ti^+$, error 7.17 ppm), 576.3 ($C_{30}H_{50}N_4P_2Ti^{+\bullet}$, error −1.72 ppm); calculated composition for [(*t*-BuN)(*t*-BuNP)]$_2$Ti(CH$_2$Ph)$_2$ is $C_{30}H_{50}N_4P_2Ti$.

[(*t*-BuN)(*t*-BuNP)]$_2$Ti(CHPh)(THF) (6). A small amount of product was precipitated as a red solid at −20 °C from the hexane extract obtained in the preparation of complex **5**. ^{1}H NMR (200 MHz, C_6D_6−CD_2Cl_2, 29 °C): δ_H 1.23 (s, 18H, *t*-Bu, P_2N_2 cycle), 1.56 (br m, 4H, THF), 1.60 (s, 18H, *t*-Bu), 3.64 (br m, 4H, THF), 4.05 (s, 1H, CHPh), 7.00−7.25 (m, 5H, Ph). ^{13}C{^{1}H} NMR (50.3 MHz, C_6D_6−CD_2Cl_2, 29 °C): δ_C 25.95 (THF), 28.54 (t, J_{PC} = 7.0 Hz, *C*H$_3$, *t*-Bu, P_2N_2 cycle), 33.84 (d, J_{PC} = 11.9 Hz, *C*H$_3$, *t*-Bu), 54.81 (t, J_{PC} = 10.5 Hz, *C*, *t*-Bu, P_2N_2 cycle), 65.6 (d, J_{PC} = 13.3 Hz, *C*, *t*-Bu), 68.00 (THF), 122.82 (Ph), 126.13 (Ph), 126.44 (Ph), 128.71 (Ph), 221.93 (d, J_{CH} = 162.9 Hz, *C*HPh). ^{31}P{^{1}H} NMR (162 MHz, C_6D_6−CD_2Cl_2, 29 °C): δ_P 115.21 (s). The structure was further confirmed by single-crystal X-ray diffraction studies.

[(2,5-*t*-Bu$_2$C$_6$H$_3$N)(*t*-BuNP)]$_2$Ti(CH$_2$Ph)$_2$ (7). [(2,5-*t*-Bu$_2$C$_6$H$_3$N)(*t*-BuNP)]$_2$TiCl$_2$ (**2**) (1.0 g, 1.36 mmol) in Et_2O (30 mL) was treated with $PhCH_2MgCl$ in THF (2 M, 1.4 mL, 2.8 mmol), as described for **5**, and the separation of the product was carried out as reported for [(*t*-BuN)(*t*-BuNP)]$_2$Ti(CH$_2$Ph)Cl. Ti complex **7** was isolated as a red solid (0.7 g; 65.5%). ^{1}H NMR (200 MHz, C_6D_6, 29 °C): δ_H 1.44 (s, 36H, *t*-BuAr), 1.57 (s, 18H, *t*-Bu), 2.91 (s, 4H, CH_2Ph), 6.82 (d, J = 7.3 Hz, 4H, Ph), 7.00 (d, 4H, J = 7.7 Hz, Ph), 7.20 (m, 4H, *t*-Bu$_2$C$_6$H$_3$), 7.38 (d, J = 8.1 Hz, 2H, Ph), 8.25 (dd, 2H, ^1J = 2.9 Hz, ^2J = 2.2 Hz, *t*-Bu$_2$C$_6$H$_3$). ^{13}C{^{1}H} NMR (50.3 MHz, C_6D_6, 29 °C): δ_C 31.0 (*C*H$_3$, 5-*t*-BuAr), 31.33 (t, J_{PC} = 6.5 Hz, *C*H$_3$, *t*-Bu), 31.54 (*C*H$_3$, 2-*t*-BuAr), 34.00 (*C*, 5-*t*-BuAr), 34.50 (*C*, 2-*t*-BuAr), 51.71 (t, J_{PC} = 13.73 Hz, *C*, *t*-Bu), 87.08 (*C*H$_2$Ph), 113.8 (Ar), 114.47 (Ar), 117.15 (Ar), 122.33 (Ph), 126.94 (Ph), 127.67 (Ph), 129.17 (Ph), 131.14 (Ar), 142.0 (d, J = 9.9 Hz, Ar), 144.00 (Ph), 150.00 (t, J = 1.2 Hz, Ar). ^{31}P{^{1}H} NMR (162 MHz, C_6D_6, 31 °C): δ_P 98.89 (s). MS(ESI): found *m*/*z* 841.5 ($C_{50}H_{75}N_4P_2Ti^+$, error 0.15 ppm), 840.5 ($C_{50}H_{74}N_4P_2Ti^{+\bullet}$, error −5.48 ppm); calculated composition for [(2,5-*t*-Bu$_2$C$_6$H$_3$N)(*t*-BuNP)]$_2$Ti(CH$_2$Ph)$_2$ is $C_{50}H_{74}N_4P_2Ti$.

[(2,6-*i*-Pr$_2$C$_6$H$_3$N)(*t*-BuNP)]$_2$Ti(CH$_2$Ph)$_2$ (8). [(2,6-*i*-Pr$_2$C$_6$H$_3$N)(*t*-BuNP)]$_2$TiCl$_2$ (**3**) (1.0 g, 1.49 mmol) in Et_2O (30 mL) was treated with $PhCH_2MgCl$ in Et_2O (1 M, 3.0 mL, 3.0 mmol), as described above, and separation of the product was carried out as reported for [(*t*-BuN)(*t*-BuNP)]$_2$Ti(CH$_2$Ph)Cl. Ti complex **8** was isolated as a red oil (0.84 g; 72.4%) ($C_{46}H_{66}N_4P_2Ti$ calcd C, 70.39; H, 8.48; N, 7.14, found C, 70.37; H, 8.65; N, 7.34). ^{1}H NMR (200 MHz, CD_2Cl_2, 31 °C): δ_H 1.42 (s, 18H, *t*-Bu), 1.47 (d, 24H, C*H*$_3$, *i*-Pr), 2.86 (two d, J_{HH} = 8.06 Hz, 4H, CH_2Ph), 3.95 (m, 4H, C*H*, *i*-Pr), 7.15−7.50 (16H, H−Ar and Ph). ^{13}C{^{1}H} NMR (50.3 MHz, C_6D_6,

29 °C): δ_C 24.18 (*C*H$_3$, *i*-Pr), 29.16 (t, *C*H, *i*-Pr), 31.36 (t, J_{PC} = 6.5 Hz, *C*H$_3$, *t*-Bu), 51.60 (t, J_{PC} = 14.5 Hz, *C*, *t*-Bu), 68.64 (*C*H$_2$-Ph), 122.24 (Ph), 123.98 (Ar), 126.89 (Ph), 129.00 (Ph), 136.37 (Ar), 140.96 (Ar), 144.43 (Ar), 146.88 (Ph). ^{31}P{^{1}H} NMR (202 MHz, C_6D_6, 21 °C): δ_P 115.68 (s). MS (EI): *m*/*z* (%) 781 (2, M^+), 695 (7, $M^+ - CH_2Ph$), 604 (10, $M^+ - 2\ CH_2Ph$), 556 (30, ligand).

[(2,5-*t*-Bu$_2$C$_6$H$_3$N)(*t*-BuNP)]$_2$Zr(CH$_2$Ph)Cl (12). [(2,5-*t*-Bu$_2$C$_6$H$_3$N)(*t*-BuNP)]$_2$ZrCl$_2$ (**10**) (0.62 g, 0.8 mmol) in Et$_2$O (30 mL) was treated with PhCH$_2$MgCl in THF (2 M, 1.0 mL, 2.0 mmol), as described above, and separation of the product was carried out as reported for [(*t*-BuN)(*t*-BuNP)]$_2$Ti(CH$_2$Ph)Cl. Complex **12** was isolated as a yellow-brown solid (0.52 g; 78.5%) ($C_{43}H_{67}N_4P_2ZrCl$ calcd C, 62.33; H, 8.15; N, 6.76, found C, 61.89; H, 8.52; N, 7.05). ^{1}H NMR (200 MHz, CD_2Cl_2, 29 °C): δ_H 1.25 (s, 18H, 2-*t*-BuAr), 1.26 (s, 18H, 5-*t*-BuAr), 1.42 (s, 18H, *t*-Bu), 3.24 (s, 2H, CH$_2$Ph), 6.74 (dd, 2H, ^1J = 6.2 Hz, ^2J = 2.2 Hz, 4-H−Ar); 6.60−7.30 (5H, Ph), 7.16 (2H, 3-H−Ar), 7.69 (dd, 2H, ^1J = 3.3 Hz, ^2J = 2.2 Hz, 6-H−Ar). ^{13}C{^{1}H} NMR (50.3 MHz, CD_2Cl_2, 29 °C): δ_C 30.85 (*C*H$_3$, 5-*t*-BuAr), 31.15 (t, J_{PC} = 6.5 Hz, *C*H$_3$, *t*-Bu), 31.34 (*C*H$_3$, 2-*t*-BuAr), 34.00 (*C*, 5-*t*-BuAr), 34.49 (*C*, 2-*t*-BuAr), 51.67 (t, J_{PC} = 13.73 Hz, *C*, *t*-Bu), 72.34 (*C*H$_2$Ph), 113.47 (Ar), 114.16 (Ar), 116.51 (Ar), 126.66 (Ph), 128.52 (Ph), 128.70 (Ph), 131.27 (Ar), 141.9 (d, *J* = 9.9 Hz, Ar), 142.18 (Ph), 149.98 (t, *J* = 1.2 Hz, Ar). ^{31}P{^{1}H} NMR (162 MHz, CD_2Cl_2, 31 °C): δ_P 97.89 (s). MS(EI): *m*/*z* (%) 829 (1, M^+), 737 (3, $M^+ - CH_2Ph$), 612 (80, ligand).

[(2,6-*i*-Pr$_2$C$_6$H$_3$N)(*t*-BuNP)]$_2$Zr(CH$_2$Ph)Cl (13). [(2,6-*i*-Pr$_2$C$_6$H$_3$N)(*t*-BuNP)]$_2$ZrCl$_2$ (**11**) (1.0 g, 1.4 mmol) in Et$_2$O (30 mL) was treated with PhCH$_2$MgCl in THF (2 M, 1.4 mL, 2.8 mmol), as described above, and separation of the product was carried out as reported for [(*t*-BuN)(*t*-BuNP)]$_2$Ti(CH$_2$Ph)Cl. Complex **13** was isolated as an orange oil (0.80 g; 74.1%) ($C_{39}H_{59}N_4P_2ZrCl$ calcd C, 60.63; H, 7.70; N, 7.25; found C, 61.09; H, 8.06; N, 6.96). ^{1}H NMR (200 MHz, CD_2Cl_2, 29 °C): δ_H 1.16 (s, 18H, *t*-Bu), 1.24 (d, 24H, C*H*$_3$, *i*-Pr), 2.46 (d, 2H, CH$_2$Ph), 3.63 (m, 4H, C*H*, *i*-Pr), 6.70−7.30 (11H, H−Ar and Ph). ^{13}C{^{1}H} NMR (50.3 MHz, CD_2Cl_2, 29 °C): δ_C 24.03 (*C*H$_3$, *i*-Pr), 29.03 (t, *C*H, *i*-Pr), 31.25 (t, J_{PC} = 6.5 Hz, *C*H$_3$, *t*-Bu), 51.58 (t, J_{PC} = 14.5 Hz, *C*, *t*-Bu), 72.41 (*C*H$_2$Ph), 121.72 (Ph), 123.71 (Ar), 128.55 (Ph), 128.72 (Ph), 136.41 (Ar), 141.11 (Ar), 144.44 (Ar), 146.38 (Ph). ^{31}P{^{1}H} NMR (162 MHz, CD_2Cl_2, 27 °C): δ_P 113.74 (s). MS (EI): *m*/*z* (%) 772 (1, M^+), 736 (3, $M^+ - Cl$), 556 (30, ligand).

[(*t*-BuN)(*t*-BuNP)]$_2$Zr(CH$_2$Ph)$_2$ (14). [(*t*-BuN)(*t*-BuNP)]$_2$ZrCl$_2$ (**9**) (1.0 g, 2.0 mmol) in Et$_2$O (30 mL) was treated with PhCH$_2$MgCl in THF (2 M, 2.0 mL, 4.0 mmol), as described above, and separation of the product was carried out as reported for [(*t*-BuN)(*t*-BuNP)]$_2$Ti(CH$_2$Ph)Cl. Complex **14** was isolated as a yellow crystalline solid (1.09 g; 89.3%) ($C_{30}H_{50}N_4P_2Zr$ calcd C, 58.12; H, 8.13; found C, 58.41; H, 7.89). ^{1}H NMR (200 MHz, C_6D_6, 29 °C): δ_H 1.27 (s, 18H, *t*-Bu, P_2N_2 cycle), 1.46 (s, 18H, *t*-Bu), 2.78 (s, 4H, CH$_2$Ph), 6.76 (t, J_{HH} = 7.33 Hz, 2H, Ph), 6.91 (d, J_{HH} = 7.0 Hz, 4H, Ph), 7.06 (t, J_{HH} = 7.33 Hz, 4H, Ph). ^{1}H NMR (500 MHz, CD_2Cl_2, 29 °C): δ_H 1.21 (s, 18H, *t*-Bu, P_2N_2 cycle), 1.33 (s, 18H, *t*-Bu), 2.45 (s, 4H, CH$_2$Ph), 6.76 (t, J_{HH} = 7.33 Hz, 2H, Ph), 6.89 (d, J_{HH} = 7.32 Hz, 4H, Ph), 7.07 (t, J_{HH} = 7.33 Hz, 4H, Ph). ^{13}C-{^{1}H} NMR (50.3 MHz, C_6D_6, 29 °C): δ_C 30.00 (t, J_{PC} = 6.5 Hz, *C*H$_3$, *t*-Bu, P_2N_2 cycle), 34.10 (d, J_{PC} = 9.2 Hz, *C*H$_3$, *t*-Bu), 54.41 (t, J_{PC} = 13.7 Hz, *C*, *t*-Bu, P_2N_2 cycle), 59.41 (d, J_{PC} = 17.2 Hz, *C*, *t*-Bu), 76.49 (*C*H$_2$Ph), 121.91 (Ph), 126.93 (Ph), 128.80 (Ph), 146.14 (*ipso*-C, Ph). ^{31}P{^{1}H} NMR (162 MHz, CD_2Cl_2, 27 °C): δ_P 106.11 (s). MS(EI): *m*/*z* (%) 527 (80, $M^+ - CH_2Ph$), 349 (90, ligand).

Generation of Cationic Species. Reaction of [(*t*-BuN)(*t*-BuNP)]$_2$Ti(CH$_2$Ph)$_2$ with B(C$_6$F$_5$)$_3$. In a glovebox a NMR tube was charged with [(*t*-BuN)(*t*-BuNP)]$_2$Ti(CH$_2$Ph)$_2$ (**5**) (55 mg, 106 μmol) and B(C_6F_5)$_3$ (54 mg, 106 μmol), after which 0.6 mL of CD_2Cl_2 was added via a syringe at room temperature and the mixture was vigorously shaken. Owing to high thermal instability and very high air and moisture sensitivity, this substance could not be isolated, and the resulting red solution was investigated only by NMR methods. ^{1}H NMR (500 MHz, CD_2Cl_2, 27 °C): δ_H 1.27−1.64 (m, 36H, *t*-Bu), 2.79 (br s, 2H, PhCH$_2$B), 2.89 (s, 2H, PhCH$_2$-Ti), 6.73 (d, *J* = 7.3 Hz, 2H, PhCH$_2$B), 6.76 (t, *J* = 7.3 Hz, 1H, PhCH$_2$B), 6.85 (t, *J* = 7.3 Hz, 2H, PhCH$_2$B), 7.1−7.5 (m, 5H, PhCH$_2$Ti). ^{31}P{^{1}H} NMR (202 MHz, CD_2Cl_2, 27 °C): δ_P 64.46 (s). ^{19}F NMR (470 MHz, CD_2Cl_2, 27 °C): δ_F −130.84 (d), −164.51 (t), −167.30 (d).

Reaction of [(2,5-*t*-Bu$_2$C$_6$H$_3$N)(*t*-BuNP)]$_2$Ti(CH$_2$Ph)$_2$ with B(C$_6$F$_5$)$_3$. In a glovebox [(2,5-*t*-Bu$_2$C$_6$H$_3$N)(*t*-BuNP)]$_2$Ti(CH$_2$Ph)$_2$ (**7**) (89 mg, 106 μmol) and B(C_6F_5)$_3$ (54 mg, 106 μmol) were mixed in a NMR tube and dissolved in CD_2Cl_2, as described for [(*t*-BuN)(*t*-BuNP)]$_2$Ti(CH$_2$Ph)$_2$ + B(C_6F_5)$_3$. Owing to high thermal instability and very high air and moisture sensitivity, the substance could not be isolated, and the resulting red solution was investigated only by NMR methods. ^{1}H NMR (500 MHz, CD_2Cl_2, 27 °C): δ_H 1.29 (s, 36H, *t*-BuAr), 1.46 (s, 18H, *t*-Bu), 2.82 (br s, 2H, PhCH$_2$B), 2.90 (s, 2H, CH$_2$PhTi), 6.74 (d, *J* = 7.3 Hz, 2H, PhCH$_2$B), 6.77 (br s, 1H, PhCH$_2$B), 6.86 (t, *J* = 7.3 Hz, 2H, PhCH$_2$B), 7.10−7.28 (m, 9H, Ar and CH$_2$PhTi), 7.74 (s, 2H, 6-H−Ar). ^{31}P{^{1}H} NMR (202 MHz, CD_2Cl_2, 27 °C): δ_P 99.00 (s). ^{19}F NMR (470 MHz, CD_2Cl_2, 27 °C): δ_F −130.84 (d), −164.45 (t), −167.26 (d).

Reaction of [(*t*-BuN)(*t*-BuNP)]$_2$Zr(CH$_2$Ph)$_2$ with B(C$_6$F$_5$)$_3$. In a glovebox [(*t*-BuN)(*t*-BuNP)]$_2$Zr(CH$_2$Ph)$_2$ (**14**) (60 mg, 106 μmol) and B(C_6F_5)$_3$ (54 mg, 106 μmol) were mixed in a NMR tube and dissolved in CD_2Cl_2 or C_6D_5Br, as described for [(*t*-BuN)(*t*-BuNP)]$_2$Ti(CH$_2$Ph)$_2$ + B(C_6F_5)$_3$. Owing to high thermal instability and very high air and moisture sensitivity, the substance could not be isolated, and the resulting orange solution was investigated only by NMR methods. ^{1}H NMR (500 MHz, CD_2Cl_2, 27 °C): δ_H 1.36 (s, 18H, *t*-Bu), 1.39 (s, 18H, *t*-Bu), 2.79 (br s, 2H, PhCH$_2$B), 3.10 (s, 2H, PhCH$_2$Zr), 6.72 (d, *J* = 7.8 Hz, PhCH$_2$B), 6.76 (t, *J* = 7.3 Hz, PhCH$_2$B), 6.84 (t, *J* = 7.3 Hz, PhCH$_2$B), 7.05−7.25 (m, PhCH$_2$-Zr and PhCH$_3$). ^{1}H NMR (200 MHz, C_6D_5Br, 27 °C): δ_H 1.20 (s, 18H, *t*-Bu), 1.32 (s, 18H, *t*-Bu), 3.10 (s, 2H, PhCH$_2$Zr), 3.29 (br s, 2H, PhCH$_2$B), 6.88−7.20 ppm (m, 10H, PhCH$_2$B and PhCH$_2$Zr). ^{13}C{^{1}H} NMR (50.3 MHz, CD_2Cl_2, 29 °C): δ_C 28.96 (m, B*C*H$_2$-Ph); 29.93 (t, J_{PC} = 6 Hz, *C*H$_3$, *t*-Bu, P_2N_2 cycle), 33.40 (d, J_{PC} = 8.4 Hz, *C*H$_3$, *t*-Bu), 55.32 (t, J_{PC} = 13.7 Hz, *C*, *t*-Bu, P_2N_2 cycle), 57.60 (d, J_{PC} = 15.6 Hz, *C*, *t*-Bu), 71.6 (Zr*C*H$_2$Ph), 122.63 (ZrCH$_2$-Ph), 125.72 (BCH$_2$Ph), 127.0 (BCH$_2$Ph), 128.86 (ZrCH$_2$Ph), 128.95 (BCH$_2$Ph), 129.46 (ZrCH$_2$Ph), 132.66 (*ipso*-*C*, BCH$_2$Ph), 135.0 (m, C_6F_5), 139.7 (m, C_6F_5), 146.22 (m, C_6F_5), 148.95 (*ipso*-*C*, ZrCH$_2$-Ph), 151.2 (m, C_6F_5). ^{13}C{^{1}H} NMR (50.3 MHz, C_6D_5Br, 29 °C): δ_C 33.6 (t, *C*H$_3$, *t*-Bu, P_2N_2 cycle), 34.40 (d, *C*H$_3$, *t*-Bu), 38.39 (m, B*C*H$_2$Ph), 54.76 (t, J_{PC} = 14.8 Hz, *C*, *t*-Bu, P_2N_2 cycle), 59.36 (d, J_{PC} = 20.5 Hz, *C*, *t*-Bu), 71.04 (Zr*C*H$_2$Ph), 122.25 (BCH$_2$Ph), 125.58 (ZrCH$_2$Ph), 128.64 (BCH$_2$Ph), 128.98 (BCH$_2$Ph), 129.2 (ZrCH$_2$Ph), 129.47 (ZrCH$_2$Ph), 134.1 (m, C_6F_5), 137.22 (*ipso*-*C*, BCH$_2$Ph), 139.1 (m, C_6F_5), 141.59 (*ipso*-*C*, ZrCH$_2$Ph), 146.2 (m, C_6F_5), 151.1 (m, C_6F_5). ^{31}P{^{1}H} NMR (202 MHz, CD_2Cl_2, 27 °C): δ_P 108.52 (s, complex **14**, traces), 103.66 (s, cation). ^{31}P{^{1}H} NMR (202 MHz, C_6D_5Br, 27 °C): δ_P 106.6 (s, complex **14**, traces), 102.1 (s, cation). ^{19}F NMR (470 MHz, CD_2Cl_2, 27 °C): δ_F −127.74 (d, B(C_6F_5)$_3$), −130.89 (d, PhCH$_2$B(C_6F_5)$_3^-$), −143.38 (s, B(C_6F_5)$_3$), −160.57 (q, B(C_6F_5)$_3$), −164.64 (t, PhCH$_2$B(C_6F_5)$_3^-$), −167.40 (d, PhCH$_2$B(C_6F_5)$_3^-$).

{[(*t*-BuN)(*t*-BuNP)]$_2$Zr(CH$_2$Ph)(Et$_2$O)}$^+$[PhCH$_2$B(C$_6$F$_5$)$_3$]$^-$ (15). In a glovebox [(*t*-BuN)(*t*-BuNP)]$_2$Zr(CH$_2$Ph)$_2$ (**14**) (120 mg, 212 μmol) and B(C_6F_5)$_3$ (108 mg, 212 μmol) were mixed in a test tube and dissolved in Et$_2$O. The reaction occurred immediately and oily material started to precipitate. The reaction mixture was separated from that precipitation and transferred into another test tube. The target product was slowly precipitated by addition of a hexane layer. All solvents were removed with a syringe, and the yellow oily

product was dried in a vacuum (210 mg; 65.6%). Owing to high thermal instability and very high air and moisture sensitivity, the substance could not be characterized by elemental analysis methods. ^{1}H NMR (500 MHz, CD_2Cl_2, 27 °C): δ_H 1.19 (CH_3 from Et_2O), 1.21 (s, *t*-Bu, P_2N_2 cycle), 1.31 (s, *t*-Bu, P_2N_2 cycle), 1.43 (s, *t*-Bu) in total 36H, 2.77 (br s, 2H, $PhCH_2B$), 2.84 (s, 2H, $PhCH_2Zr$), 3.60 (br s) and 3.76 (q, J = 7.1 Hz) 4H, CH_2 from Et_2O, 6.70 (d, J = 7.3 Hz, 2H, $PhCH_2B$), 6.75 (t, J = 7.3 Hz, 1H, $PhCH_2B$), 6.84 (t, J = 7.3 Hz, 2H, $PhCH_2B$), 7.10 (m, J = 7.63 Hz, 2H, $PhCH_2Zr$), 7.21 (m, J = 7.63 Hz, 1H, $PhCH_2Zr$), 7.42 (t, J = 7.63 Hz, 2H, $PhCH_2Zr$). ^{1}H NMR (200 MHz, C_6D_5Br, 29 °C, excess of Et_2O): δ_H 1.01 (CH_3 from Et_2O), 1.07 (d, 18H, *t*-Bu, P_2N_2 cycle), 1.18 (s, 18H, *t*-Bu), 3.23 (br s, 2H, $PhCH_2B$), 3.28 (s, 2H, $PhCH_2Zr$), 3.5 (q, CH_2 from Et_2O), 6.82 (d, J = 7.0 Hz, 2H, $PhCH_2B$), 6.96 (t, J = 7.0 Hz, 1H, $PhCH_2B$), 7.03 (t, J = 7.3 Hz, 2H, $PhCH_2B$), 7.1−7.3 (m, 5H, $PhCH_2Zr$). ^{13}C{^{1}H} NMR (50.3 MHz, C_6D_5Br, 29 °C): δ_C 13.66 (*C*H_3 from Et_2O), 30.86 (m, B*C*H_2Ph), 33.5 (t, *C*H_3, *t*-Bu, P_2N_2 cycle), 34.8 (d, J_{PC} = 10.7 Hz, *C*H_3, *t*-Bu), 58.0 (t, J_{PC} = 14.8 Hz, *C*, *t*-Bu, P_2N_2 cycle), 61.2 (d, J_{PC} = 19.5 Hz, *C*, *t*-Bu), 67.37 (*C*H_2 from Et_2O), 70.2 (Zr*C*H_2Ph), 122.25 (BCH$_2$Ph), 122.82 (ZrCH$_2$Ph), 127.13 (BCH$_2$Ph), 128.9 (ZrCH$_2$Ph), 129.03 (BCH$_2$-Ph), 129.52 (ZrCH$_2$Ph), 134.1 (m, C_6F_5), 134.8 (*ipso*-*C*, BCH$_2$Ph), 139.1 (m, C_6F_5), 146.2 (m, C_6F_5), 148.64 (*ipso*-*C*, ZrCH$_2$Ph), 151.1 (m, C_6F_5). ^{31}P{^{1}H} NMR (202 MHz, CD_2Cl_2, 27 °C): δ_P 106.4 (s). ^{19}F NMR (470 MHz, CD_2Cl_2, 27 °C): δ_F −130.94 (d, $PhCH_2B(C_6F_5)_3^-$), −164.55 (t, $PhCH_2B(C_6F_5)_3^-$), −167.37 ($PhCH_2B$-$(C_6F_5)_3^-$). MS(ESI): found *m*/*z* 527.2 ($C_{23}H_{43}N_4P_2Zr^+$, error 4.85 ppm); calculated composition for [(*t*-BuN)(*t*-BuNP)]$_2$Zr(CH$_2$Ph)$^+$ is $C_{23}H_{43}N_4P_2Zr^+$. The structure was further confirmed by single-crystal X-ray diffraction studies

Reaction of [(2,5-*t*-Bu$_2$C$_6$H$_3$N)(*t*-BuNP)]$_2$Zr(CH$_2$Ph)Cl with B(C$_6$F$_5$)$_3$. In a glovebox [(2,5-*t*-Bu$_2$C$_6$H$_3$N)(*t*-BuNP)]$_2$Zr(CH$_2$Ph)-Cl (**8**) (83 mg, 106 μmol) and B(C_6F_5)$_3$ (54 mg, 106 μmol) were mixed in a NMR tube and dissolved in CD_2Cl_2, as described for [(*t*-BuN)(*t*-BuNP)]$_2$Ti(CH$_2$Ph)$_2$ + B(C_6F_5)$_3$. Owing to high thermal instability and very high air and moisture sensitivity, the substance could not be isolated, and the resulting orange solution was investigated only by NMR methods. ^{1}H NMR (500 MHz, CD_2Cl_2, 27 °C): δ_H 1.20−1.50 (m, 54H, *t*-BuAr and *t*-Bu), 2.81 (br s, 2H, BCH$_2$Ph), 6.75 (d, J = 7.3 Hz, 2H, $PhCH_2B$), 6.77 (br s, 1H, $PhCH_2B$), 6.86 (t, J = 7.3 Hz, 2H, $PhCH_2B$), 7.14−7.26 (m, 4H, Ar), 7.74 (br s, 2H, 6-H−Ar). ^{31}P{^{1}H} NMR (162 MHz, CD_2Cl_2, 21 °C): δ_P 99.10 (s). ^{19}F NMR (470 MHz, CD_2Cl_2, 27 °C): δ_F −130.83 (d), −164.51 (t), −167.30 (d).

Polymerization Experiments. A 1 L Büchi glass autoclave was charged with 200 mL of toluene and cocatalyst (MAO or TIBA), thermostated at the required temperature, and saturated with ethene, after which the desired amount of complex solution (preliminary mixed with TIBA and B(C_6F_5)$_3$ when B(C_6F_5)$_3$ was used as the cocatalyst) was added. The benzyl complexes exhibited extremely high air and moisture sensitivity and thermal instability. To prevent the decomposition of the catalyst precursors as well as activated complexes in the presence of moisture and air traces, TIBA was added to the stock solutions of complexes (with M/TIBA ratio 1:200). The preparation of stock solutions of complexes and complex activation with B(C_6F_5)$_3$ were performed in a glovebox. The catalyst solution was introduced into an autoclave under argon pressure. The monomer pressure (±50 mbar) and reaction temperature (±0.5 °C) were kept constant during each polymerization run. Monomer consumption, polymerization temperature, and pressure were controlled by real-time monitoring. The polymerizations were quenched by pouring the resulting reaction mixture into 400 mL of methanol acidified with aqueous hydrochloric acid. After precipitation, the polymers were washed several times with methanol and water and dried at 60 °C overnight.

Single-Crystal X-ray Diffraction Studies. Crystal data of compounds **6**, **14**, and **15** were collected with a Nonius KappaCCD area-detector diffractometer at 173(2) K using Mo Kα radiation (graphite monochromator), 0.71073 Å. Data reduction: COLLECT.[8] Absorption correction: SADABS.[9] Structure solution: SHELX-97[10a] or SIR 2002,[10b] direct methods. Refinement: SHELX-97.[10a] Graphics: SHELXTL.[11] All non-hydrogen atoms were refined anisotropically. Hydrogen atoms were refined on calculated positions. In compound **6** the hydrogen atom H61a was located in a residual electron density map and refined isotropically. One disordered *t*-Bu group in **6** has two orientations with site occupation factors of 0.25 and 0.75, respectively.

Scheme 1

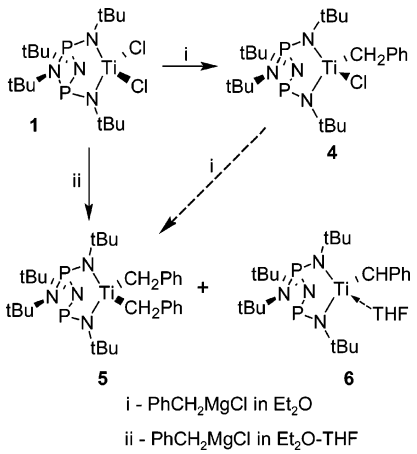

Results and Discussion

Synthesis of Benzyl Complexes. We have previously reported on the synthesis of the bulky dichloro titanium and zirconium bis(amido)cyclodiphosph(III)azane complexes.[5,6] The literature-known homosubstituted [(*t*-BuN)(*t*-BuNP)]$_2$TiCl$_2$ (**1**)[4b,5] and two titanium complexes having the bulkiest aryl substituents [(ArN)(*t*-BuNP)]$_2$TiCl$_2$ (**2**, Ar = 2,5-*t*-Bu$_2$C$_6$H$_3$; **3**, Ar = 2,6-*i*-Pr$_2$C$_6$H$_3$)[5] were chosen for the preparation of the corresponding Ti benzyl derivatives.

Alkylation reaction of [(*t*-BuN)(*t*-BuNP)]$_2$TiCl$_2$ (**1**) with $PhCH_2MgCl$ turned out to be rather sensitive to the applied solvent. When **1** was treated with 2 molar equiv of $PhCH_2$-MgCl in Et_2O at −50 °C, only monosubstituted [(*t*-BuN)(*t*-BuNP)]$_2$Ti(CH$_2$Ph)Cl (**4**) was formed, which was confirmed by ^{1}H NMR and elemental analysis (Scheme 1). In ^{1}H NMR spectrum of **4** two separate signals for the *t*-Bu groups attached to the cyclodiphosph(III)azane ring appeared, which is due to the chemical nonequivalence of these substituents. This is a result of the unsymmetric substitution pattern in monobenzyl complex **4**, which lowers its molecule symmetry to C_s. Further alkylation of **4** with 2 equiv of $PhCH_2MgCl$ in Et_2O at −50 °C gave a red sticky solid with very low yield (ca. 10%). According to ^{1}H NMR data, the resulting raw product consisted of the desired dialkylated complex, [(*t*-BuN)(*t*-BuNP)]$_2$Ti(CH$_2$Ph)$_2$ (**5**), and dibenzyl, which was formed as a side-product. Isolation and purification of **5** failed due to its thermal instability and the presence of a large amount of dibenzyl. However, pure [(*t*-BuN)(*t*-BuNP)]$_2$Ti(CH$_2$Ph)$_2$ (**5**) was obtained as a red solid with moderate yield when a tetrahydrofuran solution of benzylmagnesium chloride was used in the alkylation instead (Scheme 1).

(8) Nonius. *COLLECT*; Nonius BV: Delft, The Netherlands, 2002.
(9) Sheldrick, G. M. *SADABS*; University of Göttingen: Germany, 1996.
(10) (a) Sheldrick, G. M. *SHELX-97*; University of Göttingen: Germany, 1997. (b) Burla, M. C.; Camalli, M.; Carrozzini, G. L.; Cascarano, G.; Giacovazzo, C.; Polidori, G.; Spagna, R. *SIR 2002. J. Appl. Crystallogr.* **2003**, *36*, 1103.

Scheme 2

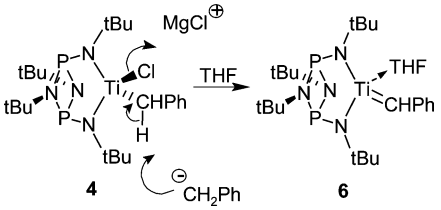

Comparison of ^{1}H NMR spectra from mono- and dibenzyl Ti complexes **4** and **5** shows that the signal of methylene hydrogens from the benzyl groups of **5** is clearly downfield shifted (3.22 vs 2.82 ppm for **4**). A similar tendency was also observed in ^{31}P NMR (129.36 ppm for **5** vs 112.35 ppm for **4**). This indicates that titanium is a stronger Lewis acid in [(*t*-BuN)(*t*-BuNP)]$_2$Ti(CH$_2$Ph)Cl (**4**) than in [(*t*-BuN)(*t*-BuNP)]$_2$Ti(CH$_2$Ph)$_2$ (**5**). This observation is in accordance with the fact that chloride is a more electron-withdrawing ligand than the benzyl group.

Surprisingly, the Ti benzylidene derivative, [(*t*-BuN)(*t*-BuNP)]$_2$Ti(CHPh)(THF) (**6**), was formed together with **5** in the alkylation reaction (Scheme 1). This side-product was sparingly soluble in hexane and was therefore separable from highly soluble [(*t*-BuN)(*t*-BuNP)]$_2$Ti(CH$_2$Ph)$_2$ (**5**). In the ^{1}H NMR of **6** the signal representing the carbene proton is shifted downfield compared to the CH$_2$ protons from the benzyl group of **5** (4.05 vs 3.22 ppm).[12] The presence of the benzylidene carbon at 221.93 ppm (J_{CH} = 162.85 Hz) in the ^{13}C NMR further confirmed the carbene nature of **6**.[13] It can be proposed that deprotonation of initially formed [(*t*-BuN)(*t*-BuNP)]$_2$Ti(CH$_2$Ph)Cl by PhCH$_2$MgCl causes Cl$^-$ elimination, which is a prerequisite to form the Ti carbene complex **6** (Scheme 2).[14] The THF coordination seems to be the driving force for this process, as in the absence of THF the reaction does not occur.

Crystals of **6** suitable for single-crystal X-ray diffraction studies were grown from the saturated hexane solution. In the solid state the titanium is pentacoordinated and adopts a distorted trigonal bipyramidal configuration wherein two amido and one cyclodiphosph(III)azane nitrogen atom, the carbon atom from the benzylidene group, and the oxygen atom from THF are located at vertexes of the coordination polyhedron (Figure 1, Tables 1 and 2). The complex exhibits C_s symmetry as a result of additional Ti−THF and Ti−N3 bondings. The Ti−CHPh bond length is short (1.901(4) Å) and clearly distinguishable from the Ti−CH$_2$Ph bond in the benzyl Ti bis(amido)complexes (in the range 2.1−2.2 Å),[15] but resembles Ti═C distances in known Ti carbene complexes.[16] Although examples of Ti carbenes have already been reported[12,13] and various benzylidene metal complexes[17] are known, this represents, to the best of our knowledge, the first defined solid-state structure of a benzylidene Ti complex.

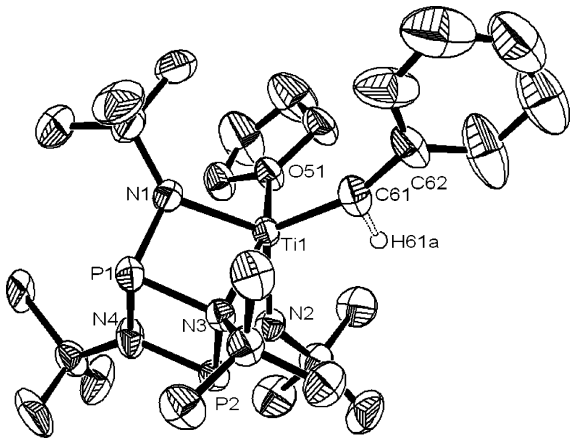

Figure 1. ORTEP plot of [(*t*-BuN)(*t*-BuNP)]$_2$Ti(CHPh)(THF) (**6**) with thermal ellipsoids drawn at the 50% probability level. Except H61a all hydrogen atoms were omitted for clarity.

Table 1. Crystallographic Data for Complexes 6, 14, and 15

	6	**14**	**15**
formula	$C_{27}H_{50}N_4OP_2Ti$	$C_{30}H_{50}N_4P_2Zr$	$C_{27}H_{53}N_4OP_2Zr$, $C_{25}H_7BF_{15}$
fw	556.56	619.90	1206.01
space group	$P\bar{1}$	$P2_1/c$	$P2_1/n$
a, Å	9.737(1)	9.067(1)	10.870(1)
b, Å	11.711(2)	18.639(3)	33.707(3)
c, Å	14.758(2)	19.798(3)	15.506(1)
α, deg	89.05(1)	90.00	90.00
β, deg	70.79(1)	77.56(1)	100.66(1)
γ, deg	89.94(1)	90.00	90.00
V, Å^3	1588.9(4)	3267(1)	5583.3(8)
d_{calc}, g cm^{-3}	1.165	1.260	1.435
Z	2	4	4
μ, mm^{-1}	0.394	0.458	0.345
λ, Å	0.71073	0.71073	0.71073
T, K	173(2)	173(2)	173(2)
R^a	0.0669	0.0336	0.0536
$R_w{}^b$	0.1728	0.0739	0.1222

^{a} $R = \sum||F_o| - |F_c||/\sum|F_o|$ for observed reflections [$I > 2\sigma(I)$]. ^{b} $R_w = \{\sum[w(F_o^2 - F_c^2)^2]/\sum[w(F_o^2)^2]\}^{1/2}$ for all data.

As electron density has moved from the metal center to the benzylidene ligand, the titanium acquires a high Lewis acid character, which materializes in the shortening of the Ti−N3 bond (2.206(3) vs 2.267(2) Å in [(*t*-BuN)(*t*-BuNP)]$_2$TiCl$_2$). The C61−H61a hydrogen was located in the Fourier electron density map and was refined isotropically. The configuration of the C61 carbene atom is highly distorted from the formal sp^2-geometry, as the angle between the Ti═C bond and Ph substituent is 163.3(5)°, and the carbene hydrogen atom is located so that the H61a−C61−Ti1 angle is about 77°. This and the relatively short

(11) Sheldrick, G. M. *SHELXTL*, Version 5.10; Bruker AXS Inc.: Madison, WI, 1997.

(12) In carbene complexes the ^{1}H NMR signal of the carbene hydrogen atom is usually considerably downfield shifted. In the case of the Ti−carbene complexes this signal was observed in the range 3−12.3 ppm. See: (a) Baumann, R.; Stumpf, W. M.; Davis, M. W.; Liang, L.-C.; Schrock, R. R. *J. Am. Chem. Soc.* **1999**, *121*, 7822, (b) Van de Heisteeg, B. J. J.; Schat, G.; Akkerman, O. S.; Bickelhaupt, F. *J. Organomet. Chem.* **1986**, *310*, C25. (c) Van der Heijden, H.; Hessen, B. *J. Chem. Soc., Chem. Commun.* **1995**, 145. (d) Basuli, F.; Bailey, B. C.; Watson, L. A.; Tomaszewski, J.; Huffman, J. C.; Mindiola, D. J. *Organometallics* **2005**, *24*, 1886, and references therein.

(13) In carbene complexes the ^{13}C NMR signal of the carbene atom is remarkably downfield shifted. In the case of the Ti−carbene complexes this signal was observed at frequencies above 200 ppm (J_{CH} in the range 80−150 Hz). See ref 12 and (a) Van Doorn, J. A.; van der Heijden, H,; Orpen, A. G. *Organometallics* **1994**, *13*, 4271. (b) Weng, W.; Yang, L.; Foxman, B. M.; Ozerov, O. V. *Organometallics* **2004**, *23*, 4700, and references therein.

(14) Carbene complex **6** formed in the alkylation reaction, and it is not a decomposition product of complex **5**. That rules out the possibility of α-elimination. Complex **5** is decomposing with formation of dibenzyl, indicating the reduction of Ti(IV).

(15) (a) Carpentier, J.-F.; Martin, A.; Swenson, D. C.; Jordan, R. F. *Organometallics* **2003**, *22*, 4999. (b) Mahanthappa, M. K.; Cole, A. P.; Waymouth, R. M. *Organometallics* **2004**, *23*, 1405. (c) Minhas, R. K.; Scoles, L.; Wong, S.; Gambarotta, S. *Organometallics* **1996**, *15*, 1113.

(16) Normal Ti═C bond lengths are in the range 1.9−2.0 Å. See refs 12, 13, and Beckhaus, R.; Santamaria, C. *J. Organomet. Chem.* **2001**, *617*−*618*, 81.

(17) (a) Groysman, S.; Goldberg, I.; Kol, M.; Genizi, E.; Goldschmidt, Z. *Organometallics* **2004**, *23*, 1880. (b) Gatard, S.; Kahlal, S.; Mery, D.; Nlate, S.; Cloutet, E.; Saillard, J.-Y.; Astruc, D. *Organometallics* **2004**, *23*, 1313. (c) Messerle, L. W.; Jennische, P.; Schrock, R. R.; Stucky, G. *J. Am. Chem. Soc.* **1980**, *102*, 6744. (d) Buijink, J.-K. F.; Teuben, J. H.; Kooijman, H.; Spek, A. L. *Organometallics* **1994**, *13*, 2922.

Table 2. Selected Structural Parameters for Complexes 6, 14, and 15

	6	14	15
		Distances, Å	
P1−N1	1.689(4)	1.6821(17)	1.720(3)
P1−N3	1.794(3)	1.7796(16)	1.799(3)
M−C	1.896(5)	2.278(2)	2.248(4)
		2.284(2)	
Zr1−C29			2.697(4)
M−N1	2.003(3)	2.1244(16)	2.094(3)
M−N2	2.015(3)	2.1120(16)	2.073(3)
M−N3	2.206(3)	2.4755(16)	2.423(3)
M−O	2.120(3)		2.243(2)
C61−C62	1.447(2)		
C51−B40			1.653(5)
C71−B40			1.682(5)
		Angles, deg	
N3−P1−N4	80.23(16)	79.24(7)	81.69(14)
N1−P1−N3	91.84(16)	93.73(8)	91.95(14)
N1−M−N2	117.38(14)	125.51(6)	117.70(11)
O−M−C	96.66(16)		85.27(13)
C17−Zr1−C24		97.71(8)	
Ti1−C61−C62	163.3(5)		
C−M−N3	107.15(17)	122.78(7)	134.16(13)
		139.15(7)	
C71−B1−C61			106.0(3)
C41−B1−C71			116.0(3)

Scheme 3

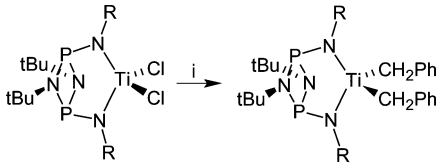

2, R - 2,5-*t*Bu$_2$C$_6$H$_3$ **7**, R - 2,5-*t*Bu$_2$C$_6$H$_3$

3, 2,6-*i*Pr$_2$C$_6$H$_3$ **8**, 2,6-*i*Pr$_2$C$_6$H$_3$

i - PhCH$_2$MgCl in Et$_2$O

Ti1−H61a distance (1.88(7) Å) indicate an agostic interaction between titanium and H61a. The C61−C62 bond is 1.445(6) Å, which is consistent with the length of standard C(sp2)−C(sp2) bonds (1.48 Å).[18] In the solid state the benzylidene group and the THF ring are almost perpendicular. The Ti−O(THF) distance is normal and 2.120(3) Å long.[19]

Bulky aryl-substituted bis(amido)cyclodiphosph(III)azane titanium complexes [(ArN)(*t*-BuNP)]$_2$TiCl$_2$ (**2**, Ar = 2,5-*t*-Bu$_2$C$_6$H$_3$; **3**, Ar = 2,6-*i*-Pr$_2$C$_6$H$_3$) were converted to corresponding moisture-, air-, and thermal-sensitive dibenzyl derivatives (**7**, Ar - 2,5-*t*-Bu$_2$C$_6$H$_3$; **8**, Ar = 2,6-*i*-Pr$_2$C$_6$H$_3$) with high yields (Scheme 3). The existence of the dibenzyl complexes **7** and **8** was validated by elemental analysis, HRMS(ESI), and ^{1}H NMR data. In the ^{1}H and ^{13}C NMR of **7** and **8** the *t*-Bu substituents at the phosph(III)azane cycle were undistinguishable from each other, and therefore in solution the C_2 molecular symmetry can be proposed for these complexes.

Alkylation of bis(amido)cyclodiphosph(III)azane Zr dichloro complexes [(RN)(*t*-BuNP)]$_2$ZrCl$_2$ (**9**, R = *t*-Bu;[4c] **10**, R = 2,5-*t*-Bu$_2$C$_6$H$_3$;[6] **11**, R = 2,6-*i*-Pr$_2$C$_6$H$_3$)[6] was carried out in conditions similar to those applied for Ti derivatives. Two equivalents of PhCH$_2$MgCl per 1 equiv of zirconium compound were used, but only monosubstituted benzyl zirconium compounds [(RN)(*t*-BuNP)]$_2$Zr(CH$_2$Ph)Cl (**12**, R = 2,5-*t*-Bu$_2$C$_6$H$_3$; **13**, R = 2,6-*i*-Pr$_2$C$_6$H$_3$) were isolated from the resulting reaction mixtures (Scheme 4). Further attempts to prepare the dibenzyl zirconium complexes were also performed by treatment of [(RN)(*t*-BuNP)]$_2$Zr(CH$_2$Ph)Cl with a 2-fold excess of PhCH$_2$MgCl. However, no desired complexes were recovered; according to ^{1}H and ^{31}P NMR data only dibenzyl and unidentified decomposition products were formed.

Scheme 4

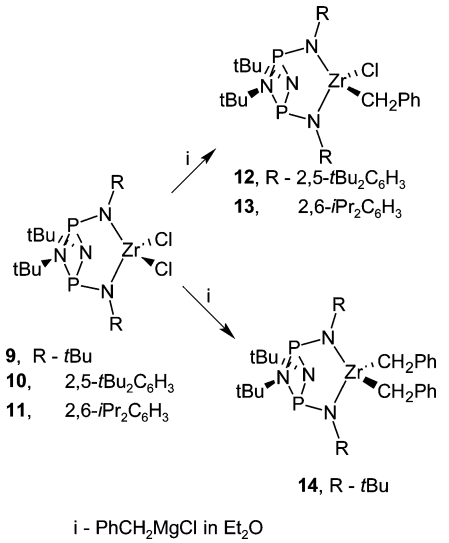

12, R - 2,5-*t*Bu$_2$C$_6$H$_3$

13, 2,6-*i*Pr$_2$C$_6$H$_3$

9, R - *t*Bu

10, 2,5-*t*Bu$_2$C$_6$H$_3$

11, 2,6-*i*Pr$_2$C$_6$H$_3$

14, R - *t*Bu

i - PhCH$_2$MgCl in Et$_2$O

On the contrary, the homosubstituted [(*t*-BuN)(*t*-BuNP)]$_2$ZrCl$_2$ (**9**) was directly converted to [(*t*-BuN)(*t*-BuNP)]$_2$Zr(CH$_2$Ph)$_2$ (**14**) with an excellent yield when treated with PhCH$_2$MgCl in Et$_2$O. According to ^{1}H NMR, **14** is C_{2v} symmetric and the Zr atom exhibits a tetrahedral configuration in solution. In the solid state the structure of **14** is analogous with [(*t*-BuN)(*t*-BuNP)]$_2$MCl$_2$ (M = Zr, Hf)[4a,c] and [(*t*-BuN)(*t*-BuNP)]$_2$HfMe$_2$.[7] In **14** the Zr atom adopts a distorted trigonal-bipyramidal configuration, which is defined by the two amido and one of the cyclodiphosph(III)azane nitrogens together with the two methylene groups from the benzyl moieties (Figure 2). The Zr−CH$_2$Ph distances (Zr1−C17 2.278(2) Å and Zr1−C24 2.284(2) Å) are in the normal range (Table 2).[20] The C−Zr−C angle (97.71(8)°) in **14** is less than the Cl−Zr−Cl angle (104.51(8)°) in the parent complex [(*t*-BuN)(*t*-BuNP)]$_2$ZrCl$_2$ (**9**)[4a] and the Me−Hf−Me angle (104.2(2)°) in [(*t*-BuN)(*t*-BuNP)]$_2$HfMe$_2$.[7]

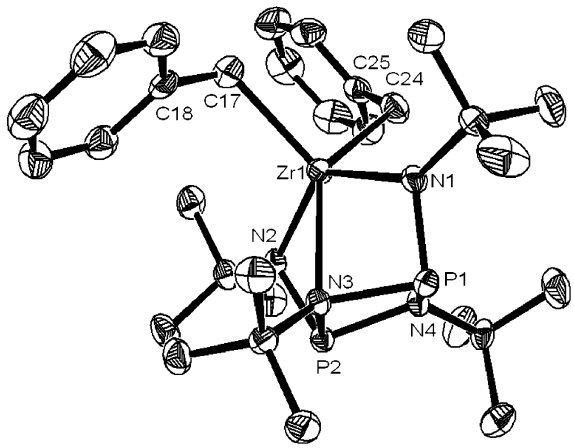

Figure 2. ORTEP plot of [(*t*-BuN)(*t*-BuNP)]$_2$Zr(CH$_2$Ph)$_2$ (**14**) with thermal ellipsoids drawn at the 50% probability level. All hydrogen atoms were omitted for clarity.

(18) March, J. *Advanced Organic Chemistry: Reactions, Mechanisms, and Structure*; Wiley: New York, 1992; p 21.

(19) (a) Li, Y.; Turnas, A.; Ciszewski, J. T.; Odom, A. L. *Inorg. Chem.* **2002**, *41*, 6298. (b) Ascenso, J. R.; de Azevedo, C. G.; Dias, A. R.; Duarte, M. T.; Eleuterio, I.; Ferreira, M. J.; Gomes, P. T.; Martins, A. M. *J. Organomet. Chem.* **2001**, *632*, 17.

Table 3. Ethene Polymerization Data for Complexes 4, 7, 8, and 12−14[a]

entry	catalyst	conc (μmol)	reaction temp (°C)	MAO/M	yield (g)	activity[b]	M_w (1)	M_w (2)
1	**4**	20	20	1000	2.9	290	2.8×10^5	
2	**4**	20	40	1000	0.7	70	4.6×10^5	
3	**4**	20	20	2000	1.5	150	5.4×10^5	9.4×10^4
4	**7**	10	20	1000	0.46	92	9.7×10^5	1.6×10^4
5	**8**	20	20	1000	1.2	120	9.1×10^5	1.5×10^4
6	**8**	20	40	1000	1.1	110	1.2×10^6	2.8×10^4
7	**8**	20	20	2000	1.1	110	1.5×10^6	6.9×10^4
8	**14**	5	20	1000	11.5	4600	4.9×10^5	2.2×10^4
9	**14**	5	40	1000	9.5	3800	4.7×10^5	2.9×10^4
10	**14**	5	20	2000	5.6	2240	5.0×10^5	2.1×10^4
11	**12**	10	20	1000	0.53	106	*c*	
12	**13**	20	40	1000	2.4	240	*c*	
13	**13**	20	40	2000	3	300	1.1×10^6	1.1×10^4

[a] 200 mL of toluene, pressure of ethylene 4 bar, polymerization time 30 min. [b] kg PE/($mol_{cat} \times h$). [c] Polymer stacked on the filters in a Waters chromatograph.

The cyclodiphosph(III)azane nitrogen−zirconium donor−acceptor interaction is weaker than in $[(t\text{-BuN})(t\text{-BuNP})]_2ZrCl_2$, which materializes in the lengthening of the Zr−N3 bond (2.4755(16) Å in **14** vs 2.398(3) Å in **9**[4c]). A similar tendency was observed in the $LHfMe_2$−$LHfCl_2$ series (L = $[(t\text{-BuN})(t\text{-BuNP})]_2^{2-}$) and can be explained by the fact that chlorine has a stronger electron-withdrawing ability than the alkyl ligands.[7] The benzyl groups are connected to zirconium in a η^1-fashion, as shown by the values of the C−C−Zr angles (C18−C17−Zr1 115.05(14)°; C25−C24−Zr1 116.17(14)°).

Ethene Polymerization Results. The synthesized $[(RN)(t\text{-BuNP})]_2M(CH_2Ph)_nCl_{2-n}$ (**4**, **7**, **8**, **12**−**14**; M = Ti, Zr; R = *t*-Bu or bulky aryl) were introduced into the ethene polymerization studies. After activation with $B(C_6F_5)_3$ (M:B ratio = 1:1) and in the presence of 500 equiv of TIBA, they showed very low polymerization activity. The reason for such marked decline in activity of the benzyl complexes compared to MAO-activated Ti and Zr dichloro analogues[5,6] could be the fast decomposition of the benzyl complexes during the activation process due to their high moisture sensitivity and thermal instability.

When MAO was used as a cocatalyst instead, moderate catalytic activities were achieved (Table 3). Despite the precautions taken (see Experimental Section), the alkyl precatalysts decomposed to a certain extent before the ethene polymerization was started. As a result, two or more kinds of catalytic species were present in the polymerization mixture, which was reflected in the bimodal molecular mass distribution of produced polymers in the GPC measurements (see Supporting Information). However, the higher molar mass fractions exhibited M_w values similar to what was observed earlier in ethene polymerization with the parent dichloro complexes under similar polymerization conditions.[5,6] The lighter molar mass fractions were most probably produced by decomposition products of the benzyl complexes.

The MAO-activated Ti and Zr complexes bearing the *t*-Bu groups (**4** and **14**, respectively) revealed very high initial activity, which, in the case of the Ti derivative **4**, severely declined after a few minutes. As a result, the overall productivity of Ti catalyst **4**/MAO was much lower than with its Zr analogue **14**/MAO (290 kgPE/($mol_{cat} \times h$) vs 4600 kgPE/($mol_{cat} \times h$)). As shown in Table 3 (runs 2, 3 and 9, 10), both complexes were also highly sensitive to the increased MAO concentration and polymerization temperature, while the Zr catalyst **13**/MAO containing very bulky 2,6-di-isopropylphenyl groups was robust against the changes in reaction conditions. **13**/MAO was approximately 3 times more active than Ti and Zr complexes having less bulky 2,5-*t*-$Bu_2C_6H_3$ substituents. Similar polymerization behavior was observed earlier for analogous dichloro Ti and Zr complexes $[(RN)(t\text{-BuNP})]_2MCl_2$ (**1**, R = *t*-Bu, M = Ti; **9**, R = *t*-Bu, M = Zr; **11**, R = 2,6-*i*-$Pr_2C_6H_3$, M = Zr); **1**/MAO exhibited high initial activity, but ethene consumption fell off sharply just after a few minutes, while **9**/MAO displayed the highest activity in the series.[5,6] Analogously, higher polymerization temperatures and MAO concentrations markedly decrease the catalytic activities of **1**/MAO and to a lesser extent **9**/MAO, while only **11**/MAO revealed increasing activity in the range of MAO/Zr ratios 500−2000 as well as in the temperature range 30−60 °C.[6] The similar trends in the polymerization behavior affirm that the structure of the actual catalytic species generated from the analogous benzyl or chloro complexes bearing the same amido substituents is similar or exactly the same regardless of the original precatalyst. This is in accordance with the generally accepted mechanism for the catalyst activation, where a dichloro complex is alkylated, and the following abstraction of the metal alkyl group by a cocatalyst leads to the formation of the catalytically active species.[21]

Generation of the Cationic Species. To generate the cationic species, the Ti and Zr benzyl complexes were involved in the reaction with $B(C_6F_5)_3$. The formation of the activated "cationic" species was followed by ^1H, ^{31}P, and ^{19}F NMR. Deuterobenzene would have been a preferable choice of solvent for the study, as it prevents complex decomposition through a stabilizing coordination to the cationic metal center.[22] Unfortunately, the generated species became insoluble in C_6D_6, and therefore further investigations were performed in CD_2Cl_2 instead. Some of the reactions were also studied in C_6D_5Br to affirm the results and to exclude possible solvent effects.

The addition of $B(C_6F_5)_3$ and CD_2Cl_2 to the yellow $[(t\text{-BuN})(t\text{-BuNP})]_2Zr(CH_2Ph)_2$ (**14**) caused a color change to orange.

(20) Zr−CH_2Ph distances found in (a) (Zr−C = 2.312(2) Å) Bazinet, P.; Wood, D.; Yap, G. P. A.; Richeson, D. S. *Inorg. Chem.* **2003**, *42*, 6225. (b) (Zr−C = 2.250(6), 2.305(7) Å) Tshuva, E. Y.; Groysman, S.; Goldberg, I.; Kol, M. *Organometallics* **2002**, *21*, 662.

(21) (a) Kaminsky, W.; Arndt, M. In *Applied Homogeneous Catalysis with Organometallic Compounds*; Cornils, B., Herrmann, W. A., Eds.; VCH: Weinheim, 1996; Vols. 1 and 2. (b) Alt, H. G.; Köppl, A. *Chem. Rev.* **2000**, *100*, 1205. (c) Brintzinger, H. H.; Fischer, D.; Mülhaupt, R.; Rieger, B.; Waymouth, R. M. *Angew. Chem.* **1995**, *107*, 1255; *Angew. Chem., Int. Ed. Engl.* **1995**, *34*, 1143.

(22) For arene coordination to group 4 metals see: (a) Doerrer, L. H.; Green, M. L. H.; Häussinger, D.; Sassmannshausen, J. *J. Chem. Soc., Dalton Trans.* **1999**, 2111. (b) Gillis, D. J.; Quyoum, R.; Tudoret, M.-J.; Wang, Q.; Jeremic, D.; Roszak, A. W.; Baird, M. C. *Organometallics* **1996**, *15*, 3600. (c) Lancaster, S. J.; Robinson, O. B.; Bochmann, M. *Organometallics* **1995**, *14*, 2456. For arene coordination to group 3 metals see: (d) Hayes, P. G.; Piers, W. E.; Parvez, W. *J. Am. Chem. Soc.* **2003**, *125*, 5622, and references therein.

In the ^{1}H NMR spectra of **14**/B(C_6F_5)$_3$ and the analogous Ti derivative **5**/B(C_6F_5)$_3$ two kinds of benzyl groups appeared due to the abstraction of one of the benzyl groups by B(C_6F_5)$_3$: B−CH_2Ph (broadened signal at 2.8 ppm, triplets at 6.84 and 6.96 ppm, and a doublet at 6.71 ppm) and M−CH_2Ph (Ti−CH_2Ph sharp peak at 2.9 ppm, Zr−CH_2Ph sharp peak at 3.1 ppm, Ph group multiplets at 7.0−7.21 ppm). Similar ^{1}H NMR spectra were also recorded for **14**/B(C_6F_5)$_3$ in C_6D_5Br. If compared to the parent complex **14**, the signal of Zr−CH_2 protons shifted 0.65 ppm downfield. Comparable ^{1}H NMR spectra were also observed for B(C_6F_5)$_3$-activated 2,5-$Bu_2C_6H_3$-substituted Ti di- and Zr monobenzyl complexes **7** and **12** (with the exception of Zr−CH_2Ph signals).

The peak of the activated "cationic" complex (103.66 ppm) was found in the ^{31}P NMR spectra of **14**/B(C_6F_5)$_3$ in CD_2Cl_2 or C_6D_5Br together with the downfield shifted signal of the unreacted parent complex (108.52 ppm). A similar shift has also been observed in the activation of [(*t*-BuN)(*t*-BuNP)]$_2$HfMe$_2$ by B(C_6F_5)$_3$ (108.3 ppm for parent complex vs 91.54 ppm for the corresponding cation).[7] The cationic species formed upon B(C_6F_5)$_3$ activation of the Ti and Zr complexes **8** and **13** bearing 2,6-*i*-$Pr_2C_6H_3$ groups appeared to be very unstable and rapidly decomposed (in a few minutes) to the corresponding phosph(III)azane ligand.

On the basis of our experience with the bis(amido)cyclodiphosph(III)azane group 4 metal complexes, the changes in the electrophilicity of the metal center after the activation can be seen in the ^{31}P NMR. The ^{31}P NMR signal of the "cationic" species is shifted upfield compared with the peak of the parent complex ($\Delta\delta_P$). On the basis of the calculated $\Delta\delta_P$ values for B(C_6F_5)$_3$-activated benzyl derivatives, the clear correlation between the catalytic activity of a certain complex and the electrophilicity of the metal center in the activated species can be established.

After activation of [(*t*-BuN)(*t*-BuNP)]$_2$Ti(CH_2Ph)$_2$ (**5**) and **14** with B(C_6F_5)$_3$, the largest $\Delta\delta_P$ in the series of investigated complexes were observed ($\Delta\delta_P$ = 65.2 ppm for **5** and $\Delta\delta_P$ = 5.0 ppm for **14**). Accordingly, the catalysts [(*t*-BuN)(*t*-BuNP)]$_2$Ti(CH_2Ph)Cl (**4**)/MAO and [(*t*-BuN)(*t*-BuNP)]$_2$Zr(CH_2Ph)$_2$ (**14**)/MAO displayed here the highest initial polymerization activity, although the activity of the former decays rapidly. Surrounded by bulky aromatic substituents, [(ArN)(*t*-BuNP)]$_2$M(CH_2Ph)$_n$Cl$_{2-n}$ (M = Ti, Zr; Ar = bulky aryl) revealed moderate activity, as well as small $\Delta\delta_P$ values (below 0.5). Presumably, the electron-rich aryl substituents donate electron density to the metal center via the amide nitrogens and diminish electron deficiency of the metal. An analogous tendency was also observed for Hf methyl complexes.[7] While [(*t*-BuN)(*t*-BuNP)]$_2$HfMe$_2$ ($\Delta\delta_P$ = 6.8 ppm) exhibited moderate activity, the related [(ArN)(*t*-BuNP)]$_2$HfMe$_2$ ($\Delta\delta_P$ = 0.5−0.7 ppm) were inactive in ethene polymerization.[23]

The abstraction of a benzyl group by B(C_6F_5)$_3$ leads to the formation of the $PhCH_2B(C_6F_5)_3^-$ anion, which often stays coordinated to the cationic complex.[24] In the ^{19}F NMR spectra of the activated complexes **5**, **7**, **12**, and **14**, regardless of the ligand substitution and the metal, the positions of the fluorine peaks in ^{19}F NMR were very similar and found around −130.9, −164.5, and −167.4 ppm with $\Delta\delta$(*m*,*p*-F) about 2.8 ppm (see Supporting Information), indicating the presence of free $PhCH_2B(C_6F_5)_3^-$ as a counterion.[25]

The full dissociation of the cationic complex−borate ion pair in CD_2Cl_2 solution leaves the metal centers in the activated species highly electrophilic. The unsaturated character of the cationic metal center can also be confirmed by their ability to coordinate additional donor ligands.[26] After addition of Me_3P to the B(C_6F_5)$_3$-activated benzyl Ti or Zr compounds **5**, **7**, **12**, and **14**, the Me_3P peak in ^{31}P NMR shifted from −60.5 ppm to the region between −6 and −20 ppm due to Me_3P coordination to the cationic metal center. At the same time no changes in the ^{19}F NMR spectrum were detected, which is consistent with the uncoordinated character of the $PhCH_2B(C_6F_5)_3^-$ anion. At ambient temperature and in the presence of a large excess of trimethylphosphine, the fast exchange between free and coordinated Me_3P can be observed in the ^{31}P NMR spectra as the broadening of the Me_3P signal (see Supporting Information). The full cation−anion dissociation and the ability of the metal in the cationic complexes to interact with donor molecules are also connected to their instability.[27]

The B(C_6F_5)$_3$-activated [(*t*-BuN)(*t*-BuNP)]$_2$Ti(CH_2Ph)$_2$ (**5**) undergoes partial decomposition during the course of the NMR experiments. The ^{1}H and ^{31}P NMR spectra of the **5**/B(C_6F_5)$_3$ showed that the decomposition was occurring via degradation of the diphosph(III)azane cycle. This is connected with the high electrophilicity of the Ti center revealed in **5**/B(C_6F_5)$_3$ (δ_P = 64.44 ppm). The donor−acceptor interactions between the highly positively charged Ti atom and the electron-rich diphosph(III)azane cycle seem to destabilize the ligand bridge against the destructive electrophilic attacks, either from neighboring cationic species or B(C_6F_5)$_3$ (in activation) or from MAO (in polymerization).

To investigate the structural chemistry of the group 4 metal bis(amido) benzyl-substituted cationic species bearing a cyclodiphosph(III)azane bridge, several attempts to crystallize the generated Ti and Zr cationic complexes were carried out. As the B(C_6F_5)$_3$-activated complexes were isolable only as oily material, the possibility to enhance the crystallization process with incorporation of an additional donor ligand was considered. Further experiments with Et_2O as a donor gave {[(*t*-BuN)(*t*-BuNP)]$_2$Zr(CH_2Ph)(Et_2O)}$^+$[$PhCH_2B(C_6F_5)_3$]$^-$ (**15**) as a yellow solid, which was very sensitive to air, moisture, and elevated temperatures. After recrystallization, crystals suitable for X-ray single-crystal diffraction studies were grown. In {[(*t*-BuN)(*t*-BuNP)]$_2$Zr(CH_2Ph)(Et_2O)}$^+$[$PhCH_2B(C_6F_5)_3$]$^-$ (**15**) the Zr atom is pentacoordinated and adopts a highly distorted trigonal-bipyramidal configuration (Figure 3, the crystal and structural parameters are in Tables 1 and 2, respectively). Two amido−zirconium bonds, Zr−N (from diphosph(III)azane cycle) and

(23) A similar tendency can be observed for other group 4 metal complexes having phosphorous atoms near the metal center. For example, for R_2TiMe_2 (δ_P = 25.72 ppm), R_2TiCl_2 (35.37 ppm), $R_2TiMe[MeB(C_6F_5)_3]$ (49.75 ppm), $R_2Ti[MeB(C_6F_5)_3]_2$ (60.57 ppm) (R = *t*Bu_3PN) the tendency is the same, but the direction for the shift of the ^{31}P NMR signal is opposite for these complexes. In the case of other Ti and Zr complexes similar data analysis can be made. See: (a) Guérin, F.; Steward, J. C.; Beddie, C.; Stephan, D. W. *Organometallics* **2000**, *19*, 2994. (b) Guérin, F.; Stephan, D. W. *Angew. Chem., Int. Ed.* **2000**, *39*, 1298. (c) Cabrera, L.; Hollink, E.; Stewart, J. C.; Wei, P.; Stephan, D. W. *Organometallics* **2005**, *24*, 1091. (d) Stephan, D. W.; Stewart, J. C.; Guérin, F.; Spence, R. E. v H.; Xu, W.; Harrison, D. G. *Organometallics* **1999**, *18*, 1116. (e) Hollink, E.; Wei, P.; Stephan, D. W. *Organometallics* **2004**, *23*, 1562. (f) Yue, N.; Hollink, E.; Guérin, F.; Stephan, D. W. *Organometallics* **2001**, *20*, 4424.

(24) Examples are: (a) Shafir, A.; Arnold, J. *Organometallics* **2003**, *22*, 567. (b) Gountchev, T. I.; Tilley, T. D. *Inorg. Chim. Acta* **2003**, *345*, 81. (c) Horton, A. D.; de With, J. *Chem. Commun.* **1996**, 1375.

(25) The value of $\Delta\delta$(*m*,*p*-F) (^{19}F NMR) is a good probe of the coordination of [$MeB(C_6F_5)_3$]$^-$ to cationic d^0 metals (values of 3−6 ppm indicate coordination; <3 ppm indicates noncoordination). See ref 24c.

(26) Schaper, F.; Geyer, A.; Brintzinger, H. H. *Organometallics* **2002**, *21*, 473.

(27) The CD_2Cl_2−LMR^+ (M = Ti, Zr, Hf) interactions were proposed in some cases based on obtained NMR data. See: Bochmann, M.; Jaggar, A. J.; Nicholls, J. C. *Angew. Chem.* **1990**, *102*, 830.

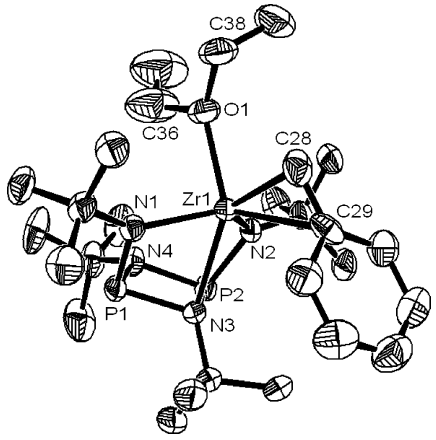

Figure 3. ORTEP plot of $\{[(t\text{-BuN})(t\text{-BuNP})]_2Zr(\eta^2\text{-}CH_2Ph)\}^+$ (**15**) with thermal ellipsoids drawn at the 50% probability level. All hydrogen atoms were omitted for clarity.

Zr−O (from Et_2O) donor−acceptor bonds, and the Zr−CH_2Ph η^2-coordination define **15** as a 16e$^-$ species.

The P_2N_2 ring is almost planar and the Zr−N3 donor−acceptor bond is shortened compared with the parent complex (2.423(3) vs 2.4755(16) Å), but not as much as in a related cationic methyl Hf complex (Hf−N was 2.315(4) Å).[7] These observations are consistent with the saturated 16e$^-$ character of complex **15**. The Zr−C28 distance is 2.248(4) Å, which is usual for Zr benzyl complexes,[19] and the Zr−C_{ipso} bond is relatively short (2.697(4) Å), indicating the Zr−η^2-CH_2Ph coordination. A similar coordination type was observed earlier;[28,29] for example in the related $[Cp_2Zr(CH_3CN)(\eta^2\text{-}CH_2Ph)]^+$ the Zr−CH_2Ph distance is 2.344(8) Å and Zr−C_{ipso} is 2.648(6) Å.[29a] The donor−acceptor Zr−O bond length in **15** is 2.243(2) Å.[30] The structure of the $PhCH_2B(C_6F_5)_3^-$ anion is ordinary (see Supporting Information).

The structures of the activated complex **14**/$B(C_6F_5)_3$ and $\{[(t\text{-BuN})(t\text{-BuNP})]_2Zr(CH_2Ph)(Et_2O)\}^+[PhCH_2B(C_6F_5)_3]^-$ (**15**) in solution were investigated by means of ^{1}H, ^{31}P, ^{13}C, and ^{19}F NMR methods. The positions of the methylene protons as well as the aromatic protons (from BCH_2Ph and $ZrCH_2Ph$ groups) in the ^{1}H NMR spectra of **15** (C_6D_5Br and CD_2Cl_2 were used as solvents) were similar to those observed for $B(C_6F_5)_3$-activated complexes **5**, **7**, **12**, and **14** (see above). In the ^{13}C NMR (C_6D_5Br) spectrum of **15**, the signal for the methylene carbon of the Zr−CH_2Ph group appears at 70.2 ppm, and the signal for the C_{ipso} atom of the Zr−CH_2Ph group was found at 148.6 ppm. Similar shifts for the carbon atoms of the benzyl group were found in the ^{13}C NMR spectra of **14**/$B(C_6F_5)_3$. Despite the Zr-η^2-CH_2Ph coordination displayed for **15** in the solid state, it can be concluded then that in solution the benzyl group coordinates to the central atom in η^1-fashion. The ^{19}F NMR data obtained for **15** confirmed that the $PhCH_2B(C_6F_5)_3^-$ counteranion is free from coordination with the cationic complex.

Conclusions

The cyclodiphosph(III)azane bis(amido) Ti and Zr benzyl complexes were synthesized, and their catalytic behavior and activation with $B(C_6F_5)_3$ were investigated. From our previous works[5,6] and present studies it appeared that they are attractive candidates for ethene polymerization, as they possess reasonable catalytic activity and the ligand framework is tunable. The Zr catalysts having a $[(t\text{-BuN})(t\text{-BuNP})]_2^{2-}$ ligand had the highest activity and metallocene catalyst-like behavior, while the Ti and Zr derivatives bearing bulky aromatic substituents gave lower productivity and produced high molecular mass polyethene. For benzyl Ti and Zr derivatives moderate up to high catalytic activities in ethene polymerization (70−4600 kg/(mol_{cat} × h)) were recorded.

Benzyl-substituted Zr complexes did not show any sign of the destruction of ligand during the activation with $B(C_6F_5)_3$. In ethene polymerization they revealed the highest average catalytic activity in the series of studied complexes. Apparently, too high electrophilicity of the cationic metal center in Ti catalysts bearing *tert*-butyl groups destabilizes the ligand framework for destructive attacks. The ligand degradation can be detected in the ^{31}P NMR, when $[(t\text{-BuN})(t\text{-BuNP})]_2Ti(CH_2Ph)_2$ (**5**) was activated with $B(C_6F_5)_3$. This is also supported by the fact that initially highly active Ti catalysts $[(t\text{-BuN})(t\text{-BuNP})]_2TiCl_2$/MAO[5] and $[(t\text{-BuN})(t\text{-BuNP})]_2Ti(CH_2Ph)Cl$/MAO rapidly become deactivated in ethene polymerization conditions.

All $B(C_6F_5)_3$-activated Ti and Zr complexes displayed their unsaturated character as they coordinate with donor Me_3P. The tendency to saturate the cationic metal center with additional donor−acceptor coordination can also be clearly established in the solid state. The $\{[(t\text{-BuN})(t\text{-BuNP})]_2Zr(\eta^2\text{-}CH_2Ph)(Et_2O)\}^+[PhCH_2B(C_6F_5)_3]^-$ is a 16e$^-$ complex due to the additional interaction with a donor nitrogen from the diphosph(III)azane cycle, the Zr−OEt_2 connection, and Zr−η^2-CH_2Ph bonding.

During the synthesis of the benzyl Ti and Zr bis(amido)-cyclodiphosph(III)azane complexes, the new Ti carbene was also isolated, and first solid-state structure of the Ti−benzylidene complex was defined.

Acknowledgment. This work was financially supported by Academy of Finland (project no. 204408 and 209739) and Finnish National Technology Agency (TEKES). Erkki Aitola is acknowledged for the GPC measurements of produced polymers.

Supporting Information Available: Listings of spectral data, GPC results, and a figure showing the structure of the $PhCH_2B(C_6F_5)_3^-$ anion. This material is available free of charge via the Internet at http://pubs.acs.org.

OM050725H

(28) Chen, E. Y.-X.; Marks, T. J. *Chem. Rev.* **2000**, *100*, 1391.

(29) For examples of the structurally characterized benzyl "cationic" complexes see: (a) Jordan, R. F.; LaPointe, R. E.; Bajgur, C. S.; Echols, S. F.; Willett, R. *J. Am. Chem. Soc.* **1987**, *109*, 4111. (b) Pellecchia, C.; Grassi, A.; Immirzi, A. *J. Am. Chem. Soc.* **1993**, *115*, 1160. (c) Pellecchia, C.; Immirzi, A.; Pappalardo, D.; Peluso, A. *Organometallics* **1994**, *13*, 3773.

(30) In the related bis(amido) Zr cation $[(MesNCH_2CH_2)_2NMe]ZrMe(Et_2O)^+$ (Mes = mesityl) the Zr−O distance is 2.234(5) Å. Schrock, R. R.; Casado, A. L.; Goodman, J. T.; Liang, L.-C.; Bonitatebus, P. J.; Davis, W. M. *Organometallics* **2000**, *19*, 5325.